Industrial Chemistry & Materials

ROYAL SOCIETY OF CHEMISTRY

PAPER

View Article Online
View Journal | View Issue

Cite this: *Ind. Chem. Mater.*, 2026, **4**, 260

Scaling up electrochemical CO_2 reduction to formate through comparative reactor analysis†

Paniz Izadi, *[a] Swapnil Varhade,[b] Carl Schneider,[a] Philip Haus,[a] Chandani Singh,[c] Avni Guruji,[b] Deepak Pant[bd] and Falk Harnisch[a]

This study presents scalable reactor designs at a lab-scale pilot level for the electrochemical CO_2 reduction reaction (eCO_2RR) to formate, utilizing formate-selective catalysts such as tin (Sn) and bismuth (Bi) at the electrodes in different sizes. Furthermore, it evaluates multiple scaled-up reactor configurations, providing critical insights into their performance, efficiency, and potential for industrial deployment. Electrochemical cells comprising VITO CORE® gas diffusion electrodes (GDEs) of 100 cm^2 single electrode, 300 cm^2 stack (3 electrodes of 100 cm^2) and 400 cm^2 single electrode were evaluated for eCO_2RR at 100 mA cm^{-2} at two different laboratories (UFZ and VITO). The 100 cm^2 Sn-GDEs showed an average formate production rate (r_{HCOO^-}) and coulombic efficiency (CE) of 29 mM h^{-1} and 80%, respectively. However, stacking three 100 cm^2 GDEs, hence stacked 300 cm^2 Sn-GDEs, showed lower performance (average r_{HCOO^-} and CE of 19 mM h^{-1} and 50%, respectively), with a variation among the replicates. Operational efficiency and stability were regained by further scaling up using a single Sn-GDE to 400 cm^2 (average r_{HCOO^-} and CE of 35 mM h^{-1} and 73%, respectively). The Bi-GDE in the similar setup of 400 cm^2 showed lower performance (average r_{HCOO^-} and CE of 23 mM h^{-1} and 63%, respectively), which we related to electrode structural degradation as revealed by SEM-EDX analyses. With its notable durability, stable performance, and relatively low overpotential for eCO_2RR, the 400 cm^2 Sn-GDE setup demonstrated strong potential for long-term eCO_2RR to formate. The corresponding power consumptions at the largest scale for formate production using both Sn- and Bi-GDEs were determined to be 190.8 and 501.8 Wh mol^{-1}, respectively. This situates the technology at the upper boundary of laboratory-scale and the early stages of pilot-scale operation. Although the system has not yet achieved kilowatt-level performance, the results underscore a promising and scalable approach toward the development of industrially relevant eCO_2RR platforms.

Received 14th April 2025,
Accepted 24th June 2025

DOI: 10.1039/d5im00056d

rsc.li/icm

Keywords: eCO_2RR; Scale up; Formate; Gas diffusion electrodes; Flow cells; Stacked reactors.

1 Introduction

Electrochemical CO_2 reduction (eCO_2RR) provides a sustainable route to produce valuable chemicals, which are up to now derived from fossil resources.[1–4] This technology offers a dual benefit: using greenhouse gas emissions as feedstock and creating economic value through the generation of products.[5,6] The versatility of the products obtained from eCO_2RR, which can be used in various industries including energy, pharmaceuticals, and agriculture, further highlights its importance.[7–10] Based on technoeconomic assessments among all the products observed in eCO_2RR, currently formate and CO are the top contenders for being commercialized.[11–13] Formate (or formic acid), produced *via* eCO_2RR, has diverse industrial applications. It is used extensively as a preservative and antibacterial agent in livestock feed, a silage additive, and as a component for leather tanning.[14–16] Additionally, formate serves as an important intermediate in chemical synthesis, including the production of pharmaceuticals, textiles, and rubber. Its use as a fuel in direct formic acid fuel cells (DFAFCs) further highlights its potential in energy storage and power generation, contributing to the development of clean energy technologies.[17–19] Moreover, the integration of CO_2 reduction technologies with renewable energy sources can enhance the efficiency and sustainability of the energy grid. By storing excess renewable electric energy in chemical form, these technologies address the intermittency issues associated with *e.g.*, wind or solar power. Overall, eCO_2RR represents a

[a] *Department of Microbial Biotechnology, Helmholtz Centre for Environmental Research (UFZ), Leipzig, Germany. E-mail: paniz.izadi@ufz.de*
[b] *Electrochemistry Excellence Centre (ELEC), Materials & Chemistry Unit, Flemish Institute for Technological Research (VITO), Boeretang 200, Mol 2400, Belgium*
[c] *Research Institutes of Sweden (RISE), Bioeconomy Division, Örnsköldsvik, Sweden*
[d] *Center for Advanced Process Technology for Urban Resource Recovery (CAPTURE), Frieda Saeysstraat 1, 9052 Zwijnaarde, Belgium*

† Electronic supplementary information (ESI) available. See DOI: https://doi.org/10.1039/d5im00056d

critical technology to combat climate change, offering a pathway to both environmental sustainability and circular economy.[20]

The development and utilization of technologies related with eCO_2RR to formate have been explored over the past few years to accelerate transition.[21] While many advances in eCO_2-RR to formate have been demonstrated at the lab-scale ($\leq$10 cm^2) as summarized in Table 1, the transition towards larger, industrially relevant scales is a critical ongoing challenge. Different strategies on preparing stable and active catalysts for eCO_2RR as well as continuous production of formate or formic acid through eCO_2RR have been explored.[22,23] In addition, Orlić *et al.* (2024)[8] reported on formic acid synthesis for hydrogen storage and Belsa *et al.* (2024)[5] provided a comprehensive analysis of the current state as well as future prospects of CO_2 electroreduction technologies. The latter emphasized the need for standardized protocols, interdisciplinary collaboration, and the adoption of insights from mature technologies such as water electrolysis and fuel cells to overcome existing challenges and accelerate the transition from laboratory research to industrial-scale applications.[5] These studies highlight the significant potential for advancement but also the hurdles that need to be overcome in terms of efficiency, stability, and cost. In this context, the scalability of electrode materials is a key for advancing eCO_2RR to formate, towards industrial feasibility. Scalable electrodes, such as large-area Sn and Bi electrodes, ensure that the processes can be upscaled from laboratory settings to industrial applications, enabling high throughput and efficient production.[24] This scalability is essential to meet the demands of reducing substantial quantities of CO_2 and producing significant amounts of formate as required for making the process economically viable.

To date, the performance metrics such as coulombic efficiency (CE) for eCO_2RR to formate have been achieved mainly at the lab-scale, even across various reactor configurations.[25] Nevertheless, the development of an electrolyser for eCO_2RR to formate at the industrial scale remains unreported. In particular long-term stability studies, so far, have reported issues such as catalyst leaching, poisoning, and Ostwald ripening as the reasons for catalyst degradation.[15] These electrode stabilization issues have been addressed in our previous lab-scale studies,[24,26] using in-house prepared self-sustaining metal-based gas diffusion electrodes (GDEs). Using tin (Sn) and bismuth (Bi) as the catalysts, the GDEs were operated for an industrially relevant duration ($\geq$1000 h) at a current density of 100 mA cm^{-2} for eCO_2RR to formate. An initial activation *via* electrochemical sintering enhanced the electrode performance. Following stable operation beyond 600 h, reactivation was achieved through anodic pulsing and electrolyte solution renewal.[24] These studies had distinguished the degradation causes, to optimize the stability test up to several thousand hours.

In another study, we performed eCO_2RR to formate using a similar 10 cm^2 Sn-GDE and evaluated the system performance.[27] For that study, we used a flow cell and connected the cathode compartment thereof to a tank reservoir with 0.5 L catholyte, where formate accumulated, and performed the complete electron and carbon balances. Due to the high formate-selectivity of Sn electrodes, *ca.* CE of 85% was achieved for eCO_2RR to formate, with side products being CO (*ca.* 9%) and H_2 (*ca.* 6%). We showed that by adjusting the CO_2 flow rate close to its theoretical minimum required for eCO_2RR (*ca.* 16 mL min^{-1}), a carbon conversion efficiency (CCE) of *ca.* 41% was achieved, which is very close to the theoretical maximum value of CCE of 50%.

This study explored the scale-up of eCO_2RR processes based on the promising lab-scale (10 cm^2 GDE) performance of this setup. Different reactor configurations were designed and tested. Using the identical Sn-GDE electrode material, the setup was stepwise scaled up by 10 and 30 times (the latter as a stack) at UFZ and by 40 times at VITO laboratories resulting in electrode sizes of 100, 300, and 400 cm^2, respectively, and their performance was assessed with a focus on CE, formate production, power consumption per mole of formate, and the technical features at each setup. Additionally, to show transferability of the setup to other materials, a Bi-GDE was tested at the largest scale and compared with the Sn-GDE at the same scale.

Pioneering efforts in scaling up are emerging. For instance, Det Norske Veritas (DNV)[28] developed a semi-pilot-sized reactor with a 600 cm^2 electrode area, achieving 60% CE towards formate with 96 hours of stability. Another notable example includes the work by Fink *et al.* (2024)[12] who reported on a 3052 cm^2 electrochemical flow cell achieving 62% CE for formate production. Our current study contributes to this scaling-up effort by evaluating various reactor configurations up to 400 cm^2. Specifically, our 400 cm^2 Sn-GDE achieved an average CE of approximately 73% for formate production over 5 hours of operation with a notable rate for formate production. These encouraging results compare favourably in terms of CE and electrode size with some of the reported semi pilot scaled-up systems, while also reinforcing the notion that ensuring long-term stability, consistent performance across different scales (as seen with our stacked 300 cm^2 system), and overall energy efficiency remain key areas for intensive research and development. This work aims to provide critical insights into the practical challenges and performance metrics encountered during such scaling endeavours.

2 Results and discussion

2.1 100 cm^2 Sn-GDE setup performance

100 cm^2 Sn-GDEs were first activated by applying a cell voltage of up to 12 V and monitoring current. After achieving stable current (*ca.* 45 ± 5 A) over almost an hour, the electrodes were activated, and eCO_2RR was further performed for 2 h by fixing the current at 10 A. As expected at the Sn electrodes, formate was the main product with a CE of almost 80% during 2 h of operation (Fig. 1). This value was slightly lower than the CE achieved using the same GDE at a

10-fold smaller scale (87.3 ± 0.9% after 2 h).[27] The electrons not used for eCO_2RR to formate were used for production of CO and H_2 with respective CEs of 6.5 ± 0.8% and 5.5 ± 0.3% (Table S1†), being also in the same range when compared to respective 6.8 ± 0.5% and 5.1 ± 1.4% at 10 cm^2 Sn-GDEs after 2 h. Notably, the formate production rate (r_{HCOO^-}) achieved at the 100 cm^2 Sn-GDEs of 29.2 ± 2.3 mM h^{-1} was comparable with the rate at the 10 cm^2 Sn-GDEs (32.5 ± 2.8 mM h^{-1}), when the ratio of electrode surface area to catholyte volume was maintained constant.[27] Additionally, the CCE at 100 cm^2 Sn-GDEs being 41.7 ± 1.1% was very similar to that at 10 cm^2 Sn-GDEs (40.6 ± 1.8%). Both values are close to the theoretical maximum CCE under alkaline and biocompatible conditions. This maximum CCE is 50%, as CO_2 needs to convert stoichiometrically equally to formate and bicarbonate under these conditions. It is worth mentioning that pH and conductivity, which are important parameters in eCO_2RR, did not change remarkably during the experiment (Fig. S1†), from *ca.* 7.5 and 43 mS cm^{-1} at the beginning to *ca.* 8.2 and 52 mS cm^{-1} at the end of operation, respectively. This stability can be attributed to the duration and the sufficient catholyte volume in the tank reservoir.

These results show that 10-fold scale-up from 10 cm^2 to 100 cm^2 of the Sn-GDE setup did not significantly decrease the CE and CCE or r_{HCOO^-}, which is often observed by scale-up. However, the cell voltage and hence energy efficiency of the system seemed to be affected. Cell voltage during eCO_2RR at 10 cm^2 Sn-GDEs was stable at *ca.* 4.0 V, while this was increased to an average value of 6.2 V during the operation at 100 cm^2 Sn-GDEs, indicating higher internal resistance of the reactors by scaling up most likely due to the higher electrode gap at the larger scale GDE reactors (4–8 mm) compared to that at the 10 cm^2 GDE reactors (1–2 mm). Over 2 h eCO_2RR operation to formate, the final formate titre of 2.7 g L^{-1} was achieved, and a power consumption of 360 Wh mol^{-1} was calculated (see Table S2† for detailed calculations).

2.2 300 cm^2 Sn-GDE setup performance

Based on the successful 10-fold scale-up to 100 cm^2 of the Sn-GDE setup, numbering up was implemented to enhance CO_2 conversion capacity. Thus, instead of using a single 300 cm^2 electrode, three 100 cm^2 electrodes were used in a stack and connected in series in terms of electric connection and liquid flow. Only during the activation process was each electrode activated individually by connecting the 100 cm^2 GDE separately to the power supply. This ensured the successful activation of each electrode similar to their single use before.

One of the challenges in the stacked configuration during eCO_2RR was maintaining a similar and constant CO_2 pressure and flow across the stack. To achieve this, instead of feeding all compartments together—which led to irregular CO_2 distribution—each gas compartment of the 100 cm^2 GDE was connected to a separate rotameter and CO_2 inlet, while the outlet of each chamber was closed to establish a flow-through configuration. This ensured better control of CO_2 pressure and inlet flow in each electrode chamber. The 2-hour experiments were performed in four replicates to account for the observed variations across different operations. Although formate was still the major product of eCO_2RR, its concentration was lower than that produced using 100 cm^2 Sn-GDE reactors. During the 2 h experiment, an average r_{HCOO^-} and CE of 18.7 ± 5.2 mM h^{-1} and 50.1 ± 15.0%, respectively, were achieved, reaching the final formate titre of 3.1 g L^{-1}. Thereby, the maximum r_{HCOO^-} of *ca.* 25 mM h^{-1} corresponded to *ca.* 70% CE, and the minimum r_{HCOO^-} of *ca.* 12 mM h^{-1} corresponded to *ca.* 34% CE, hence the high standard deviation during the experiment (Fig. 2). Although the CE for H_2 production in 10 and 100 cm^2 Sn-GDE setups was around 5%, this was much higher (between 15% and 34%) at the stacked 300 cm^2 Sn-GDE setup.

Similar to the previous scale (100 cm^2 GDE), catholyte pH and conductivity changed only from *ca.* 7.6 and 43 mS cm^{-1} at the beginning to *ca.* 8.3 and 58 mS cm^{-1} at the end of operation, respectively (Fig. S2†). In addition, over 2 h eCO_2RR operation, the cell potential at this setup was in average 6.2 V, similar to that at the 100 cm^2 GDE setup and the power consumption per mole of formate was calculated to be 397 Wh mol^{-1} (see Table S3† for detailed calculations).

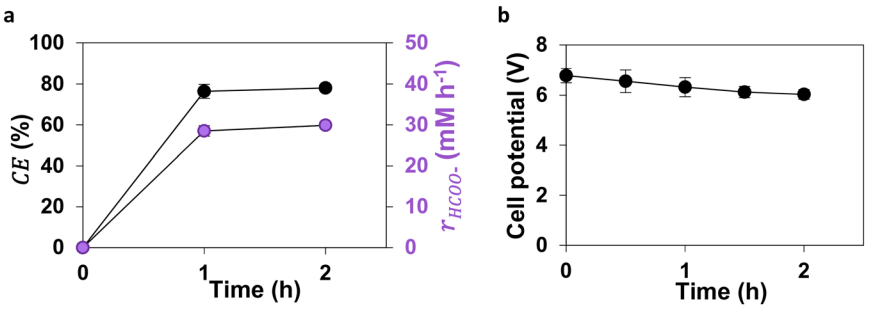

Fig. 1 (a) Coulombic efficiency (CE) for formate production, formate production rate (r_{HCOO^-}), and (b) cell potential during 2 h eCO_2RR operation at the triplicate 100 cm^2 Sn-GDE reactors (n = 3) at the applied current of 100 mA cm^{-2}, catholyte solution of 0.5 M $KHCO_3$, anolyte solution of 3 M KOH and use of CEM.

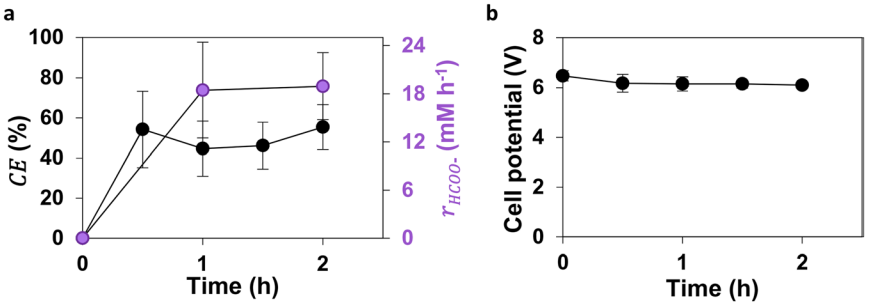

Fig. 2 (a) Coulombic efficiency (CE) for formate production, formate production rate (r_{HCOO^-}), and (b) cell potential during 2 h eCO_2RR operation at the quadruplicate stacked 300 cm^2 Sn-GDE reactors (n = 4) at the applied current of 100 mA cm^{-2}, catholyte solution of 0.5 M $KHCO_3$, anolyte solution of 3 M KOH and use of CEM.

2.3 400 cm^2 Sn-GDE setup performance

The GDEs were further scaled up to 400 cm^2 in a single reactor. After activation, eCO_2RR was performed for 5 hours. The CE for formate production remained above 80% during the first 3 hours, confirming the selectivity of the Sn-GDE towards formate. However, it dropped to around 50% between 3 and 5 hours of operation (total CE of 73.4 ± 12.2% throughout the experiment). The total concentration of formate produced (including the formate migration to the anolyte) reached up to 8 g L^{-1}, with an r_{HCOO^-} of 35.8 ± 11.5 mM h^{-1}. The decrease in system performance after 2–3 h of eCO_2RR could be due to the catalyst degradation as indicated by the increase in oxidised Sn-species at the electrode over time observed from SEM and EDX analyses (section 2.5).

The Sn-GDEs operated at a stable cell potential of 3.0–3.5 V throughout the experiment (Fig. 3). This stability in cell potential suggests that the Sn electrodes maintained good conductivity and minimal overpotential, even after prolonged use. The low overpotential for eCO_2RR at Sn is consistent with its high CE for formate production, indicating efficient charge transfer and minimal energy losses. The power consumption over 5 h eCO_2RR to formate at the Sn-GDE was calculated to be approximately 190.8 Wh mol^{-1} (see Table S4† for detailed calculations), demonstrating the potential of this setup for further pilot-scale implementation.

2.4 400 cm^2 Bi-GDE setup performance

Building on the successful operation of the 400 cm^2 Sn-GDEs, a different catalyst was also tested at this scale to further validate the reactor performance and show transferability of the results. Since Bi is also known as a formate selective electrocatalyst in eCO_2RR,[29,30] 400 cm^2 Bi-GDEs were assessed.

The eCO_2RR at Bi-GDEs showed a CE of 80% for formate production after 1 h operation, however after that it dropped more rapidly than that at the Sn-GDE, reaching *ca.* 59% and 45%, after 3 h and 5 h, respectively (Fig. 4). The r_{HCOO^-} was almost stable at an average of *ca.* 37 mM h^{-1} only for the first two hours of operation and decreased to *ca.* 13 mM h^{-1} and 11 mM h^{-1} after 3 h and 5 h, respectively. This resulted in a decrease of the overall CE and r_{HCOO^-} to 63.1 ± 14.1% and 22.8 ± 12.4 mM h^{-1}, respectively, over the 5 h operation, reaching the total final formate concentration (including that migrated to anolyte) of 5.1 g L^{-1}. These results showed that Bi-based catalysts may have suffered from faster degradation compared to Sn-based catalysts. This was also suggested by the changes observed at the surface morphology through SEM and EDX images which is discussed in section 2.5.

In contrast to the 400 cm^2 Sn-GDE reactor, the cell potential of the 400 cm^2 Bi-GDE started at 4.5 V, increased slowly and reached almost 8.0 V after 5 h operation. This increase in overpotential correlated with the observed

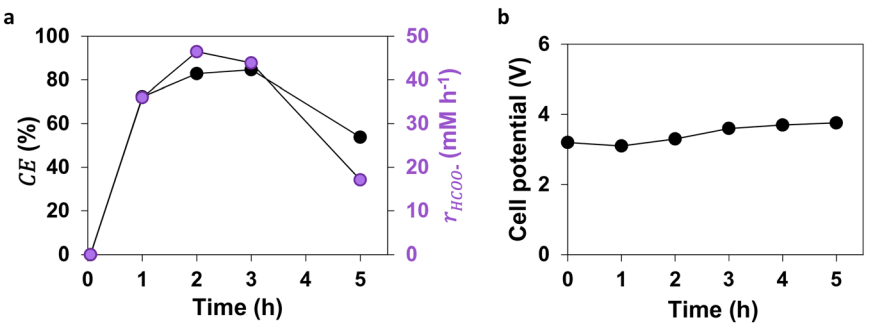

Fig. 3 (a) Coulombic efficiency (CE) for formate production, formate production rate (r_{HCOO^-}), and (b) cell potential during 5 h eCO_2RR operation at the 400 cm^2 Sn-GDE reactor (n = 1) at the applied current of 100 mA cm^{-2}, catholyte solution of 2 M KOH, anolyte solution of 2 M KOH and membrane of AEM.

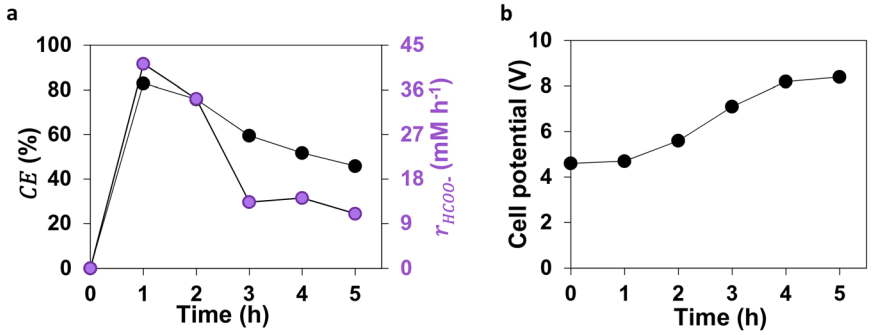

Fig. 4 (a) Coulombic efficiency (CE) for formate production, formate production rate (r_{HCOO^-}), and (b) cell potential during 5 h eCO_2RR operation at the 400 cm^2 Bi-GDE reactor (n = 1) at the applied current of 100 mA cm^{-2}, catholyte solution of 2 M KOH, anolyte solution of 2 M KOH and membrane of AEM.

degradation in CE and suggested that the Bi electrodes suffered from increased resistance and lower charge transfer efficiency as the surface degraded. The higher overpotential for the Bi-GDE compared to the Sn-GDE means that more electric energy is required to maintain the same reaction rate, making Bi less energy-efficient than Sn for long-term eCO_2RR. Over 5 h operation, the power consumption for eCO_2RR to formate at the Bi-GDE was calculated to be approximately 501.8 Wh mol^{-1} (see Table S4† for detailed calculations), more than two times than that calculated at the 400 cm^2 Sn-GDE.

2.5 Differences of Sn- and Bi-GDEs in large scale setups

Since catalyst degradation and release of metal (ions) to the electrolyte solution was observed during the experiments, SEM and EDX analyses were performed to compare the changes in surface structures (Fig. S3–S6†).

Initially, the Bi electrode had a rough and porous surface, providing sufficient active sites for CO_2 adsorption and reduction (Fig. 5c and S3†). After 5 hours of operation, the surface appeared smoother, with a reduction in the initial surface features, suggesting some structural changes and some degree of material degradation (Fig. 5d and S4†). This structural degradation was likely due to Bi leaching into the electrolyte solution, which reduced the number of active sites available for eCO_2RR.[30,31] As a result, the r_{HCOO^-} declined more rapidly in the Bi-GDE reactor than in the Sn-GDE reactor. Comparing the SEM images of the Sn electrode before and after 5 h operation (Fig. 5a and b), a decrease in surface roughness as well as porosity was observed (details in Fig. S5†), which also suggested that electrode degradation

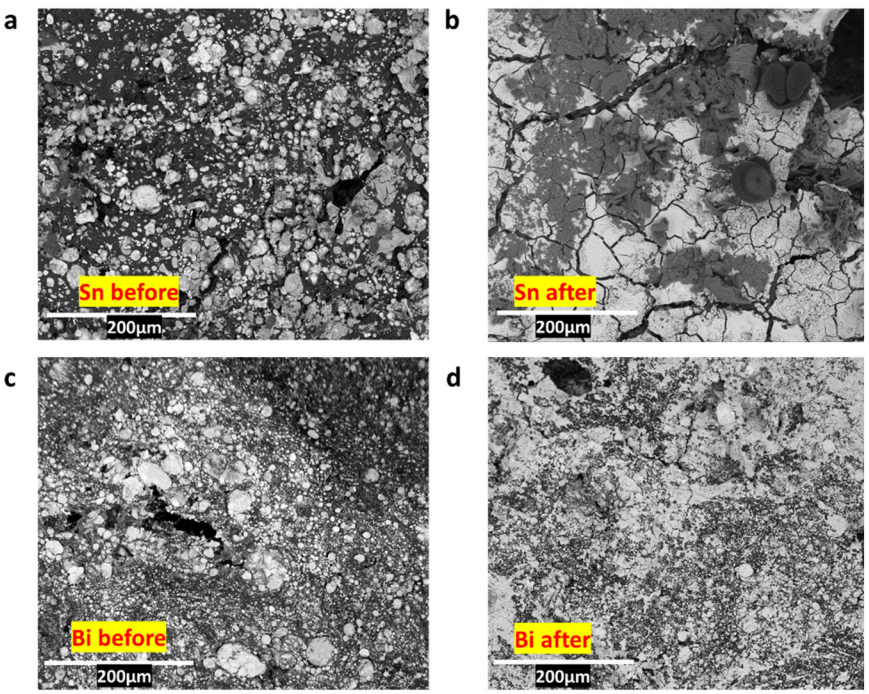

Fig. 5 SEM images of Sn electrodes (a) before and (b) after, and Bi electrodes (c) before and (d) after the 5 h eCO_2RR operation at the 400 cm^2 Bi- and Sn-GDE reactors (n = 1) at the applied current of 100 mA cm^{-2}, catholyte solution of 2 M KOH, anolyte solution of 2 M KOH and use of AEM.

reduced the active sites available for CO_2 adsorption. In addition, the comparison of elemental mapping *via* SEM-EDX analysis showed an increase in oxygen content at all the electrodes after the experiment (Fig. S6 and S7†), indicating formation of oxides.[32–34] The pH fluctuations of the catholyte were more pronounced with the Bi electrode, with a stronger decrease in pH towards the end of the experiment (reaching pH *ca.* 8). This larger shift in local pH may have contributed to the faster decline in CE, as it can affect reaction kinetics and CO_2 solubility. These changes along with formation of bicarbonate salts are known to lower CO_2 diffusion to the catalytic sites, thus impacting the performance slightly after prolonged use.[30] Nevertheless, the Sn electrode displayed greater structural integrity over the course of the experiment, with only minor degradation, while the Bi electrode exhibited more rapid performance decline due to surface smoothening and material loss. The higher stability of the Sn electrode could be attributed to the stronger Sn–CO_2 interaction, which could promote more efficient and selective formate production. Intrinsic properties of Sn lead to both good catalytic performance for formate (potentially due to Sn–CO_2 interaction) and separately, better operational stability under the tested conditions compared to Bi. The observed greater structural integrity of the Sn electrode compared to the Bi electrode could therefore be attributed to a combination of factors: potentially lower intrinsic leachability of Sn (or its oxides being formed *in situ*) under reaction conditions compared to Bi, or better adherence and compatibility of the Sn particles within the PTFE-based GDE matrix. In contrast, the Bi electrodes are more prone to surface degradation reducing the active surface area and leading to faster performance decay.

Catholyte and anolyte solutions for 400 cm^2 GDE setups were 2 M KOH, which provides a highly alkaline and conductive environment for eCO_2RR. The anolyte (KOH solution) was maintained at around pH 13, while the catholyte pH decreased over time due to the consumption of hydroxide ions during the eCO_2RR (Fig. S8†). It is known that carbonate and bicarbonate salt formation can consume the hydroxide ions in catholyte solution.[11] For both Sn and Bi electrodes, the pH of the catholyte decreased over time, likely due to the consumption of hydroxide ions during the eCO_2RR (Fig. S8†), which affected CE and r_{HCOO^-}. For Bi electrodes, the pH fluctuations were more pronounced, with a greater decrease in pH towards the end of the experiment reaching the pH of *ca.* 8. This larger shift in pH may have contributed to the faster decline in CE observed when Bi electrodes were used, as changes in the local pH can affect the reaction kinetics and CO_2 solubility.[35,36]

The high ionic conductivity of the KOH electrolyte ensured efficient charge transfer during the electrochemical reaction, with no significant drops in performance due to electrolyte depletion. However, the pH changes observed over time suggest that periodic electrolyte refreshment or at least pH-static operation is necessary for long-term operation.

2.6 Upscaling flow cell GDE reactors for eCO_2RR: performance and comparisons

eCO_2RR to formate is one of the promising pathways to convert CO_2 to a valuable product that can be used as feedstock for further synthesis. To incite this eCO_2RR to formate to industrial applications, the scale up and numbering up of setups are first required to be designed, developed and evaluated. In this study, large-scale flow cell GDEs (≥100 cm^2 electrodes) were operated for eCO_2RR in different configurations in different laboratories and compared with our previous lab-scale operation (Fig. 6) as well as other studies (Table 1). This comparative study evaluated the scalability of the GDEs and reactor designs developed and operated in two different laboratories, with differences in operating conditions (particularly catholyte pH). These slight differences need to be considered when directly comparing performance metrics such as CE and r_{HCOO^-} across all scales. The 100 cm^2 and stacked 300 cm^2 GDE reactors were operated with a cation exchange membrane (CEM) (Fumasep FKS-PET-130) and used 0.5 M $KHCO_3$ as the catholyte during eCO_2RR. The pH of the $KHCO_3$ catholyte was adjusted to approximately 7.5 by CO_2 purging before the experiments. The 400 cm^2 GDE reactors were operated with an anion exchange membrane (AEM) (Fumasep® FKB-PK-130) and used 2 M KOH as the catholyte during eCO_2RR. This created a highly alkaline environment, with the anolyte pH around 13, and the catholyte pH also starting high and decreasing over time. The choice of conditions for the 400 cm^2 setup (2 M KOH, AEM) reflects a common approach for bulk electrolysis aiming for high current densities and conductivity, whereas the $KHCO_3$ system represents conditions often explored for more pH-neutral operations.

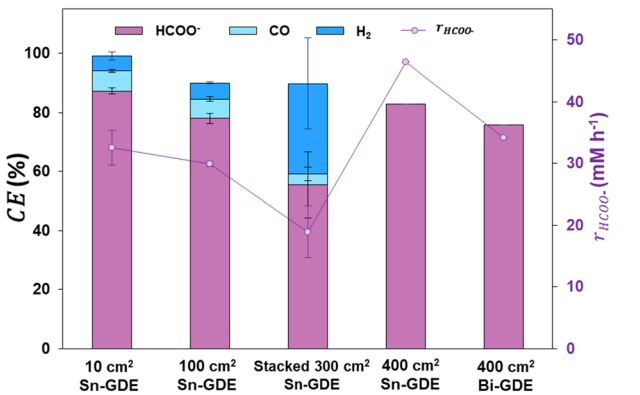

Fig. 6 Comparison of coulombic efficiency (CE) for all the products and formate production rate (r_{HCOO^-}) after 2 h of eCO_2RR in the reactors with 10 cm^2 Sn-GDE from our previous work (n = 3),[27] 100 cm^2 Sn-GDE (n = 3, catholyte: 0.5 M $KHCO_3$, anolyte: 3 M KOH, membrane: CEM), stacked 300 cm^2 Sn-GDE (n = 4, catholyte: 0.5 M $KHCO_3$, anolyte: 3 M KOH, membrane: CEM), 400 cm^2 Sn-GDE (n = 1, catholyte: 2 M KOH, anolyte: 2 M KOH, membrane: AEM) and 400 cm^2 Bi-GDE (n = 1, catholyte: 2 M KOH, anolyte: 2 M KOH, membrane: AEM). H_2 and CO were not measured in the 400 cm^2 GDE reactors.

Table 1 Comparison of eCO_2RR to formate in flow cell gas diffusion electrode setups

Reference	Cathode size (cm^2)	Current density (mA cm^{-2})	Average CE for formate (%)	Catalyst	Length of operation (h)	Average final formate concentration (g L^{-1})	Power consumption (Wh $mole^{-1}$)
33	1	450	90	Sn_3O_4	2.5	N.A.	N.A.[a]
34	3	236	94	In-doped SnO_x	14	N.A.	N.A.[a]
38	5	50	65	Sn	54	N.A.	N.A.[a]
39	5	140	94	Sn NPs	142	90	N.A.[b]
Our previous study[27]	10	100	87 ± 1	Sn	2	2.8	212
40	10	150	70	Sn NPs	1.5	2.5	N.A.[b]
41	10	200	80	Bi	1.5	4.0	277
42	25	500	90	SnO_2	10	N.A.	N.A.[a]
This study	100	100	79 ± 1	Sn	2	2.7	360
This study	300 (3 stacks of 100)	100	50 ± 15	Sn	2	3.1	397
This study	400	100	73	Sn	5	8.0	190.8
This study	400	100	63	Bi	5	5.1	501.8
12	3052	200	62 ± 4	Sn	1.5	9.0	450

N.A.: not applicable.[a] The exact formate concentration is not available. [b] The exact catholyte solution volume is not available.

In the largest scale setup (400 cm^2 GDEs), we also compared the performance of Sn and Bi, two electrocatalysts being selective for eCO_2RR to formate. Due to a technical issue, no gaseous products were detected at the 400 cm^2 GDE setups and only formate in a wide range was quantified. In addition, the sensitive analytical techniques such as NMR and GC-MS were not used in this study to detect trace by-products. However, since identical Sn electrodes used at the 100 and 300 cm^2 GDE setups were also used in this setup, it is reasonable to expect that similar by-products, such as CO and H_2, at similar shares were generated. Additionally, based on previous studies using Bi-GDEs for eCO_2RR,[2,3] CO and H_2 are again the expected by-products alongside formate. The results show that upscaling is achievable at performance metrics comparable with lab-scale. Formate was the main product in all GDEs and the CE for formate production and r_{HCOO^-} remained almost stable, except in the stacked configuration. In the stacked 300 cm^2 Sn-GDEs, the CE for formate production was the lowest, and the replicates did not show consistent performance. The challenges associated with this setup are discussed in section 2.7.

The scaled-up GDE reactors used in this study demonstrated a comparable CE to those reported in previous studies (Table 1). As observed in earlier studies, increasing the GDE size from 1 cm^2 to over 100 cm^2 resulted in a slight decrease in CE, a typical and expected trend during scale-up. Notably, scaling up Sn- or Bi-based GDEs (and therefore the reactor size) or increasing the applied current density led to higher final formate concentrations (Table 1). This increase in productivity was accompanied by a rise in power consumption. The current work with the 400 cm^2 Sn-GDE reactor demonstrated a CE of 73% towards formate with a power consumption of 190.8 Wh mol^{-1} over 5 hours. These results are competitive with our previous 10 cm^2 Sn-GDE reactor showing 87% CE with the power consumption of 212 Wh mol^{-1}.[27] Notably, we achieved higher energy efficiency at the lower current density of 100 mA cm^{-2} compared to a recently reported large-scale 3052 cm^2 cathode setup, which showed 62% CE and 450 Wh mol^{-1} at 200 mA cm^{-2} over 1.5 hours.[12] A comparison of the power consumption per mole of formate produced *via* eCO_2RR in our experiments with previous reports confirms this trend. Importantly, the power consumption values for our scaled-up reactors remained comparable to those in the literature, highlighting the feasibility and promise of the system for further scale-up leading potentially even to commercial applications.

Although a large number of studies on eCO_2RR to formate at GDE setups have been reported over the past few years, the majority of these studies were performed on a small scale ($\leq$10 cm^2 electrodes). More efforts are needed to achieve lab-scale performance metrics for large-scale GDE electrolysers. This will help identify issues and address them to commercialize the technology in the coming years.[37]

2.7 Upscaling flow cell GDE reactors for eCO_2RR: practical challenges

The upscaling of the flow cell GDE reactor in this study presented several challenges, primarily related to electrode durability, stability, and the complex configuration of the reactors. For example, a key challenge in further scaling up from 10 cm^2 GDE reactors was the need to adjust gas pressure and flow rate as a result of the increased gas chamber volume. Catalyst leaching from the GDE into the catholyte was consistently observed across all scales, evidenced both visually and through microscopic imaging, which showed catalyst detachment and dispersion. Long-term operation also showed issues with salt formation (*e.g.*, bicarbonate, carbonate or potassium hydroxide) being a common problem in eCO_2RR systems.[43] Multiple factors could influence mass transport, current and potential distribution, local pH, and CO_2 utilization, thereby affecting

overall cell efficiencies and contributing to performance decay when not optimally managed at larger scales.

Although a highly alkaline catholyte was used in the 400 cm^2 GDE setups to mitigate this, pH decline over time still led to salt generation, further exacerbated by anion crossover as well as migration through the AEM to the anode compartment. Flooding of the gas compartment was occasionally observed due to significant pressure differences across the large electrode, which were manually corrected during the experiment but would benefit from an automated feedback loop in extended operations. In addition, the large electrode size increased flow resistance, causing greater pressure losses as gas was distributed over a larger surface area – and potentially higher energy need for gas pressurising, resulting in pressure drop across the electrodes during the electrolyser operation.

Comparing single-GDE reactors to a stacked 300 cm^2 GDE configuration revealed additional complexity: uniform CO_2 distribution across compartments was not achievable with a single inlet, necessitating the use of three separate rotameters. Despite product quantification *via* HPLC and inline micro-GC, the system's overall CE remained below 80%, potentially due to product leakage or other inefficiencies (*e.g.*, heat loss) inherent to the stacked design. Notably, CE for H_2 production was higher in this configuration, indicating a shift in reaction selectivity. Lastly, inconsistent performance among replicates pointed to instability in the reactor's technical operation, further highlighting the challenges of numbering up. These can be potentially improved by precise monitoring and stabilising the gas pressure at each gas chamber.

Long-term stability of the GDE electrolysers without varying the performance metrics has been the major challenge. The long-term stability of the GDEs for operation over 1000 h was demonstrated in our previous lab-scale study.[24,26] Initial electrochemical sintering activated the electrodes, and stable operation beyond 600 hours was maintained, with reactivation achieved *via* anodic pulsing and electrolyte solution renewal.[24,26] In addition, we believe the aforementioned challenges such as electrode activity, catalyst leaching, and H_2 evolution due to pH change as well as other reasons such as formate poisoning of the catalysts could be the main reasons for lack of long-term stability of the eCO_2RR performance in flow cell GDE reactors. Formate poisoning of the catalysts refers to the potential phenomenon where the formate product, or species derived from it, adsorbs strongly onto the active catalytic sites, thereby blocking these sites from accessing CO_2 reactant molecules. Moreover, CO_2 humidification is an important factor for long-term operation, as it enhances GDE durability and helps preventing salt formation on the electrode. This can be achieved by recycling unconverted CO_2 from the catholyte headspace, which also contains moisture. This approach not only humidifies the CO_2 but also improves carbon conversion efficiency. In order to overcome these issues, more studies on upscaled reactors (>100 cm^2 electrodes) over long-term operation (>5 h) and their performance optimisation are required, similar to the scaling-up efforts underway for industrial water electrolysis for hydrogen production.[44,45]

3 Conclusions

In this study, the flow cell gas diffusion electrode (GDE) reactor for the electrochemical CO_2 reduction reaction (eCO_2RR) to formate was successfully scaled up in two different laboratories. Upscaling our previous 10 cm^2 GDE setup 10, 30 and 40 times, comparable performance in terms of coulombic efficiency (CE) and formate production rate (r_{HCOO^-}) was observed. When single Sn-GDEs of 100 cm^2 and 400 cm^2 were used for eCO_2RR operations, CE and r_{HCOO^-} were almost similar, with a r_{HCOO^-} of more than 30 mM h^{-1} and CE of 80%, respectively. The 300 cm^2 GDEs were operated by stacking three 100 cm^2 Sn-GDEs. Although formate was still the major product from CO_2, compared to other reactors more electrons (*ca.* 25%) were converted to H_2. This could be due to the complexity of the stacked reactor and difficulty to control the gas pressure between the stacks. In addition, eCO_2RR at the 400 cm^2 GDE was operated using Bi as a catalyst which showed lower stability of the catalyst and higher overpotential over time compared to when Sn was used at this scale. Furthermore, the corresponding power consumptions at the largest scale for formate production using both Sn- and Bi-GDEs were determined to be 190.8 and 501.8 Wh mol^{-1}, respectively. Given its superior stability, the Sn-GDE is a strong candidate for scaling up to sizes of at least 400 cm^2, with larger setups offering valuable opportunities for further exploration and optimization in future studies. This positions the systems presented here at the upper boundary of laboratory-scale development and at the initial phase of pilot-scale operation. Thus, a comprehensive assessment of its energy efficiency remains a subject for future investigation.

4 Experimental

4.1 Gas diffusion electrode preparation

Sn- and Bi-GDEs were fabricated following the established protocol detailed elsewhere,[26] using a sequential layer-by-layer methodology. The gas diffusion layer (GDL) and catalyst layer (CL) were independently prepared and subsequently integrated to produce a unified GDE (Fig. 7). The catalyst precursors, Sn powder (99.8%, 325 mesh, Alfa Aesar) in the case of Sn-GDE, and Bi powder (99.5%, 325 mesh size, Thermo Scientific Chemicals) in the case of Bi-GDE were separately mixed with polytetrafluoroethylene (PTFE, Dupont, 669N X) in a 70 : 30 mass ratio using a K-mix (Microtron MB 550, KINEMATICA AG, Switzerland) technique. Each mixture was compacted into a cuboidal structure (dimensions: 10 cm × 10 cm × 5 cm) using a hydraulic press (AC Hydraulics A/S 20 ton capacity) under controlled conditions of 26 ± 5 °C and 20-ton pressure.

The compacted materials underwent calendaring, wherein they were processed through progressively pressurized cold-rolled metal rollers (custom made at VITO), resulting in a

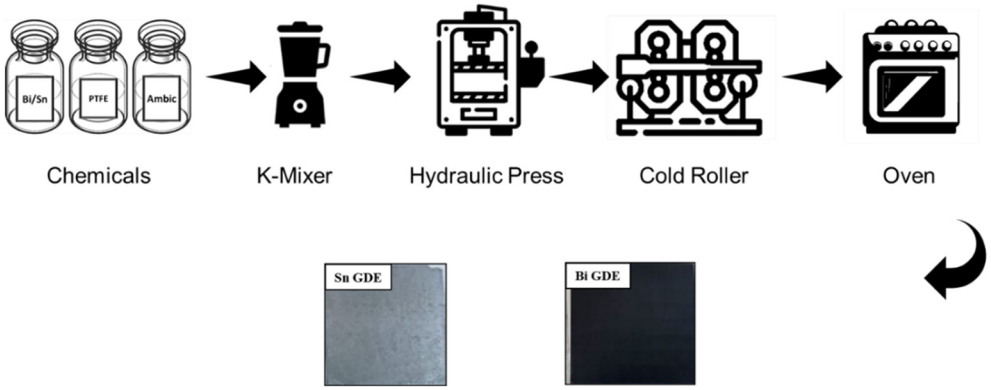

Fig. 7 Pictorial scheme for the GDE preparing process (details in the text).

uniform sheet with a final thickness of 0.5–0.6 mm, encompassing both the GDL and CL components. To achieve a cohesive and mechanically stable electrode structure, the GDL and CL were laminated through additional calendaring steps. The assembled GDE was thermally treated in an oven (WTC binder FD720) at 70 °C for 6 h to eliminate residual moisture and enhance porosity, forming the final Sn- and Bi-GDE architecture.

The processed sheets, trimmed to specified dimensions, were manufactured at scales of up to 23 cm × 23 cm. These electrodes were subsequently employed in different scale reactors at VITO as well as UFZ, with an active geometric area of 10, 100 and 400 cm^2.

4.2 Reactors and setups

4.2.1 100 cm^2 GDE reactors. The 100 cm^2 GDE reactor setup (Fig. 8) was established and operated at UFZ laboratories, by 10-fold scaling up the previous lab-scale GDE setup,[27] keeping the ratio of electrode surface to catholyte volume constant at 20 cm^2 L^{-1}. The reactor was a customised commercial reactor purchased from ElectroCell® (Electro MP Cell, Denmark). The cell comprised two titanium current collectors—one with a perforation pattern for a Sn-GDE (cathode), designed to allow gas flow through the electrode and the other for the platinised titanium anode (ElectroCell®, Denmark, 100 cm^2)—PTFE middle plates, gaskets and end plates. Each cathodic and anodic compartment had a net volume of 100 mL and were separated by a cation exchange membrane (CEM, Fumasep FKS-PET-130, FUMATECH BWT GmbH, Bietigheim-Bissingen, Germany). Each compartment was connected to a separate tank reservoir for the recirculation. A 5 L Duran bottle (DWK Life Sciences GmbH, Germany) was used as a tank reservoir for the catholyte recirculation using a peristaltic pump (Masterflex® Ismatec®, flow of 100 mL min^{-1}). The bottle

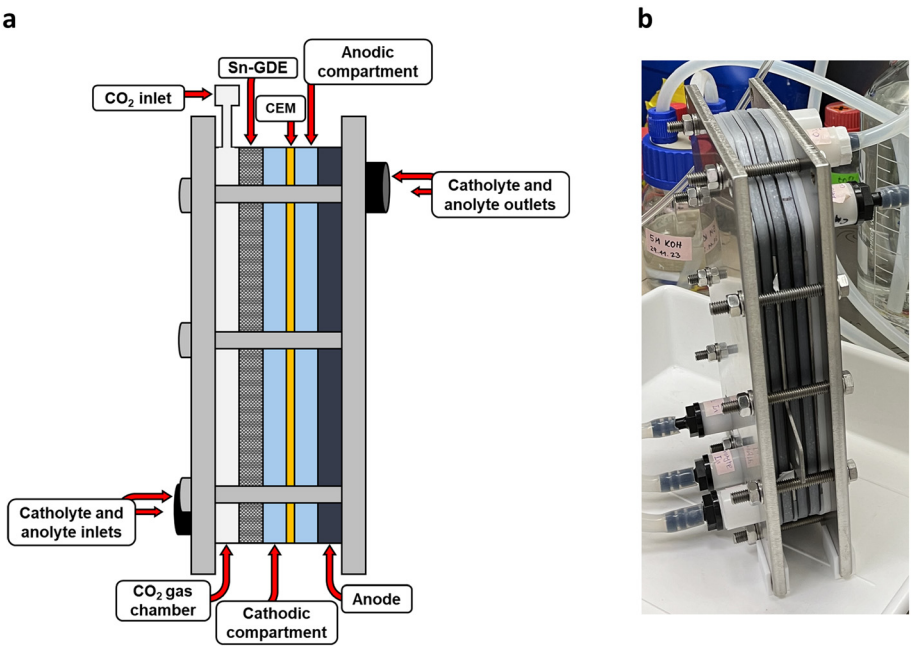

Fig. 8 (a) Schematic and (b) image of the 100 cm^2 GDE reactor used in this study.

was designed with 6 extra ports for 1) catholyte inlet, 2) catholyte outlet, 3) pH probe, 4) conductivity probe for continuous measuring, 5) a gas sampling port connected to a mass flow meter and a micro gas chromatograph (micro GC) for the inline gas detection (details in section 4.5), and 6) a liquid sampling port (Fig. S9†), similar to the previous setup.[27] The pH and conductivity were measured using a SevenExcellence S470 (Mettler-Toledo, Greifensee, Switzerland) with an InLab Micro Pro pH probe and an InLab 710 conductivity probe (both Mettler-Toledo, Greifensee, Switzerland), respectively. Both probes were calibrated using commercial buffer solutions (Mettler-Toledo, Greifensee, Switzerland) before each experiment. A 1.0 L Duran bottle (DWK Life Sciences GmbH, Germany) with 2 extra ports for the anolyte recirculation using a peristaltic pump (Masterflex® Ismatec®, flow of 100 mL min^{-1}) was used as a tank reservoir for the anolyte. The system was operated and kept gas tight, and the solutions were stirred using two magnet stirrers at 1000 rpm during the experiments. Liquid sampling was performed every 1 h by collecting 2 mL of the electrolyte solutions.

Gaseous CO_2 (Air Products GmbH, 99.5%, 1 bar) was fed to a CO_2 rotameter (VAF-Fluid-Technik GmbH) and then to the gas chamber of the reactor in the back side of the GDE. The CO_2 flow rate was adjusted at 160 ± 15 mL min^{-1} throughout the experiment, which slightly exceeded the minimum theoretical amount required when considering the electrons provided (for details see also our previous study),[27] and the gas outlet at the gas chamber was blocked to operate the experiments under flow through conditions.

A DC power source (2230-30-1 triple Channel DC Power Supply, Keithley/Tektronix GmbH, Köln, Germany) was used to fix the current during eCO_2RR at 100 mA cm^{-2} which means 10 A for the 100 cm^2 GDE between the cathode and anode, and the respective cell voltage was monitored. For the GDE activation, the cell voltage (up to 12 V) was applied at the electrode and the current was monitored. The negative and positive current of the DC power supply was connected to the cathode and anode, respectively. The experiments were conducted in triplicate (n = 3).

4.2.2 300 cm^2 GDE reactors. The 300 cm^2 GDE reactor setup (Fig. 9) was established and operated at UFZ, by stacking three 100 cm^2 GDEs. The reactor was a customized commercial reactor purchased from ElectroCell® (Electro MP Cell, Denmark). The cell comprised six titanium current collectors, three with a perforation pattern for Sn-GDEs as cathodes designed to allow gas flow and three others for the platinised titanium anode (ElectroCell®, Denmark, 100 cm^2), PTFE middle plates, gaskets and end plates. Each stack comprised one Sn-GDE and one anode separated by a cation exchange membrane (CEM, Fumasep FKS-PET-130, FUMATECH BWT GmbH, Bietigheim-Bissingen, Germany). Three stacks were sandwiched together using the end plates, while the stacks were separated from each other using an end gasket. The three Sn-GDEs were connected to each other using a braided copper wire (16 mm^2 cross sectional area, length of 20 cm, wire spec: H07V-K) to act as one cathode (Fig. 9b), while the three platinized anodes were connected to each other using a separate wire to act as one anode. Each cathodic and anodic compartment of one stack had a net volume of 100 mL being connected by tubes resulting in a net volume of cathodic and anodic chamber of the whole setup of 300 mL each, which were connected to separate tank reservoirs for recirculation. A 15 L Duran bottle (DWK Life Sciences GmbH, Germany) was used as a tank reservoir for the catholyte recirculation using a peristaltic pump (Masterflex® Ismatec®, flow of 200 mL min^{-1}) to keep the electrode surface/catholyte volume similar to the 100 cm^2

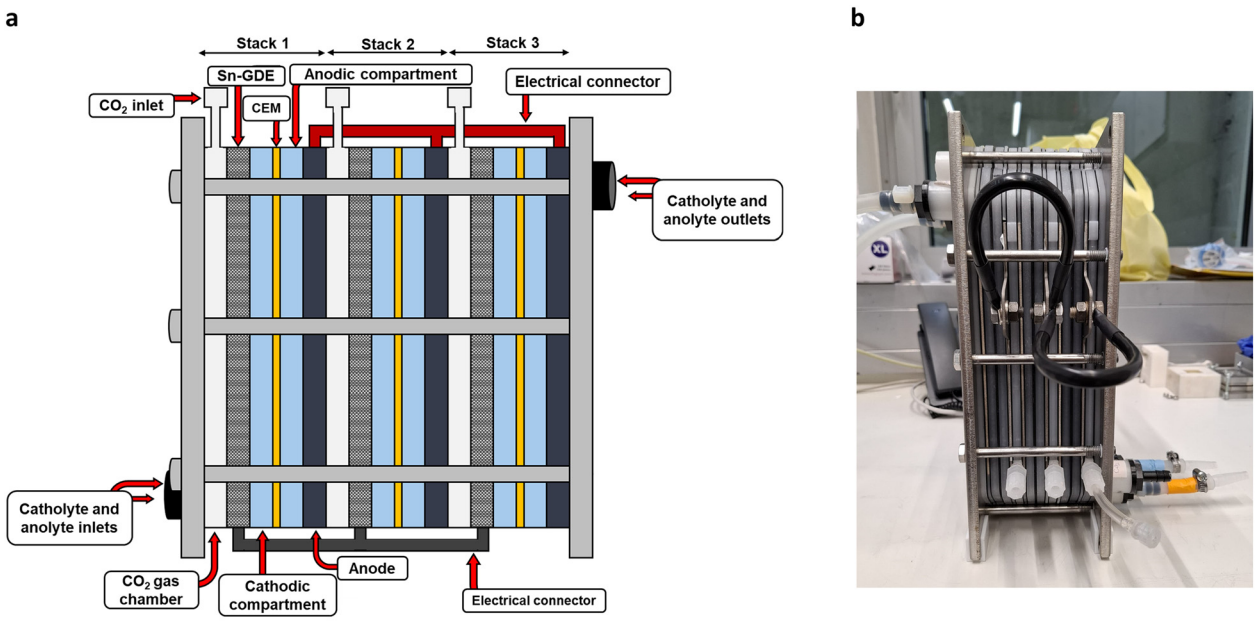

Fig. 9 (a) Schematic and (b) image of the stacked 300 cm^2 GDE reactor used in this study.

GDE setup (20 cm^2 L^{-1}). The bottle was designed with 4 extra ports for 1) catholyte inlet, 2) catholyte outlet, 3) a gas sampling port connected to a mass flow meter and a micro GC for the inline gas detection (details in section 4.5), and 4) a liquid sampling port (Fig. S10†), similar to the 100 cm^2 GDE setup. Due to the limitations caused by the size of the bottle, pH and conductivity probes were not inserted; instead they were measured separately after each liquid sampling. Similar pH and conductivity probes as well as the micro GC and mass flow meter used in the 100 cm^2 GDE reactors were also used in this setup. A 5 L Duran bottle (DWK Life Sciences GmbH, Germany) with 2 extra ports for the anolyte recirculation using a peristaltic pump (Masterflex® Ismatec®, flow of 200 mL min^{-1}) was used as a tank reservoir for the anolyte. The system was operated and kept gas tight, and the solutions were stirred using two magnet stirrers at 1000 rpm during the experiments. Liquid sampling was performed every 30 minutes by collecting 5 mL of the electrolyte solutions.

Gaseous CO_2 (Air Products GmbH, 99.5%, 1 bar) was fed to the system. In order to control the CO_2 flow rate within the stack configuration of the reactor, each gas chamber was connected to one CO_2 rotameter (VAF-Fluid-Technik GmbH) using a 3-way gas port and each gas flow was adjusted at 160 ± 15 mL min^{-1}, leading to the total CO_2 flow of *ca.* 480 mL min^{-1} throughout the experiment. The outlet of the gas line at the reactor was blocked to operate the experiments under flow through conditions.

A DC power source (2230-30-1 triple Channel DC Power Supply, Keithley/Tektronix GmbH, Köln, Germany) was used to fix the current during eCO_2RR at 100 mA cm^{-2} which means 30 A for the stacked 300 cm^2 GDE between the cathode and anode, and the respective cell voltage was monitored. To ensure a similar voltage distribution across each electrode, the voltage of the electrodes was monitored separately every 15 min using a manual digital multimeter (RS-Pro 14, UK). For the GDE activation, the cell voltage (up to 12 V) was applied at each electrode and the current was monitored. The negative and positive current of the DC power supply was connected to the cathode and anode, respectively. The experiments were conducted in quadruplicate (n = 4).

4.2.3 400 cm^2 GDE reactors. The 400 cm^2 GDE reactor setup (Fig. 10) was established and operated at VITO. The cell consisted of structural rings made of polysulfone (PSU) and polyoxymethylene (POM), including 2 PSU rings at the end of each structural plate and 3 POM rings, all sealed with O-rings made of EPDM (Ethylene Propylene Diene Monomer) (Fig. S11†). Unless specifically mentioned, all the cell components were custom developed at VITO. A titanium current collector with a titanium ring was used to hold the GDEs, and a polyoxymethylene (POM) plastic structure ring/separator with 2 cm thickness was introduced to ensure mechanical stability. The anolyte chamber consisted of a nickel (Ni) plate with a Ni spring (Rhodius Abrasives GmbH, Burgbrohl, Germany) and Ni felt (Bekaert, Zwevegem, Belgium) placed on the plastic POM. VITO-made Sn- and Bi-GDEs were used as cathodes (details in section 4.1). Each anodic and cathodic compartment was separated by an anion exchange membrane (Fumasep® FKB-PK-130, FUMATECH BWT GmbH, Bietigheim-Bissingen, Germany). The anolyte and catholyte in a separate 15 L tank reservoir were recirculated using a pump (IWAKI MX-250CV5E) at 145.2 L h^{-1}. pH and conductivity probes were installed in the tanks for an inline

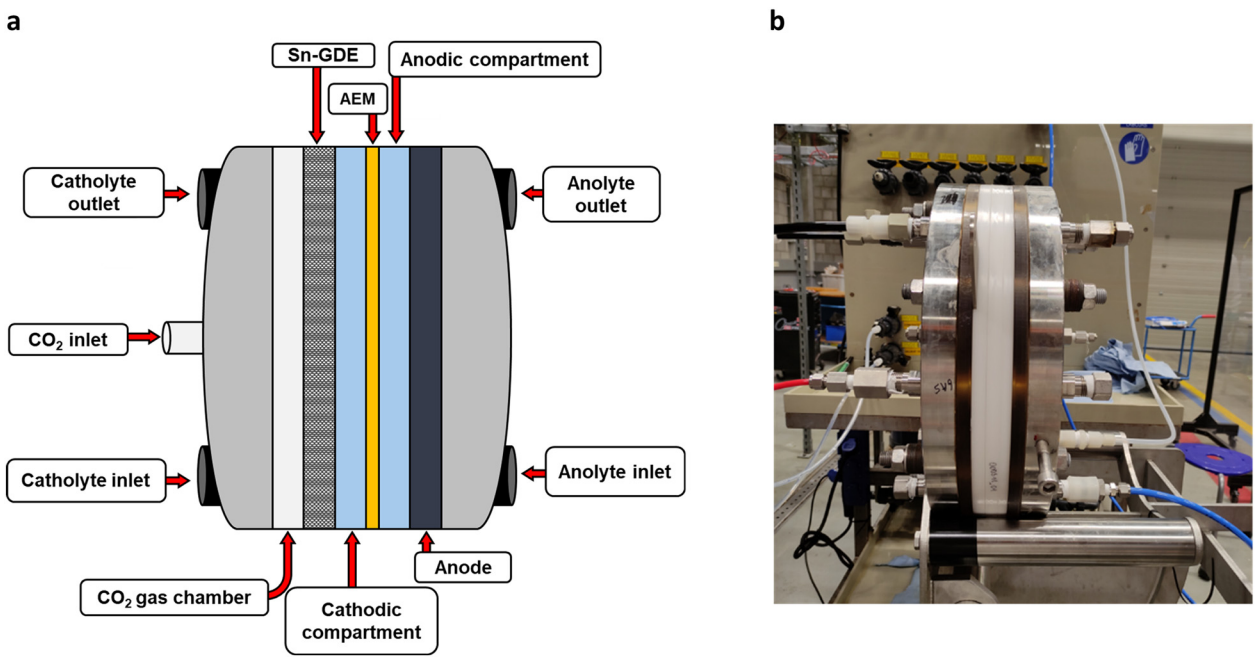

Fig. 10 (a) Schematic and (b) image of the 400 cm^2 GDE reactor used in this study.

measurement. Liquid sampling was performed every 1 h by collecting 15 mL of the electrolyte solutions.

Gaseous CO_2 (UHP grade, Air products, Belgium) was fed to the gas chamber of the reactor at the back side of the GDE. The CO_2 flow rate was adjusted between 800–1000 mL min^{-1} throughout the experiment, depending on the gas pressure at the inlet and outlet. A much higher CO_2 flow rate was used to ensure stable operation of the setup, as a reliable sufficient gas supply was critical for the performance of the single large electrode. During the GDE activation, N_2 was provided using flow through mode by adjusting the back pressure of the GDE using a manometer (RS PRO, RS-8890). The pressure differential was monitored and adjusted at both the inlet and outlet to prevent flooding in the gas chamber.[12] The inlet pressure was always kept at 0.05–0.1 bar higher than the outlet. During the eCO_2RR, flow through mode was applied by closing the gas outlet, to ensure all the CO_2 in the system was preserved. A DC power source (E-A Electro-Automatik GMbH & Co. EA-PSI 9080-170, Viersen, Germany) was used to fix the current during eCO_2RR at 100 mA cm^{-2} which means 40 A for the 400 cm^2 GDE between the cathode and anode, and the respective cell voltage was monitored. For activation, the cell voltage (up to 12 V) was fixed and the current was monitored. The negative and positive current of the DC power supply was connected to the cathode and anode, respectively.

The set up was build using the magnetically coupled pumps (IWAKI MX-250CV5E, Tessenderlo, Belgium), pH meters (Elscolab Knick Stratos, Kruibeke, Belgium), conductivity meters and temperature sensors (Elscolab Knick Stratos, Kruibeke, Belgium), pressure gauge (E&H; CerabarMPMC51, Reinach, Switzerland), flow meters (Rotameter type from GEMÜ, Ingelfingen, Germany), diaphragm valve and filters (Georg Fischer, Schaffhausen, Switzerland) in a workstation (Fig. S12†). No replicate was performed for this setup.

4.3 Electrode activation

4.3.1 GDE activation step. Before eCO_2RR operation, activation of all the GDEs was required.[24] This step re-organises the metal surface and active sites and results in a higher electric conductivity of the electrode surface.[24] Activation of GDEs was performed with N_2 gas flow instead of CO_2. Sequential increase of cell potential was applied starting from 3 V and slowly increased up to 12 V until a current of 0.3–0.6 A cm^{-2} was achieved. After that the electrodes were ready for eCO_2RR.

4.4 Anolytes and catholytes

4.4.1 Anolytes and catholytes. During GDE activation, the catholytes used at the reactors with 100, 300 and 400 cm^2 GDEs were 300 mL of 0.5 M $KHCO_3$, 500 mL of 0.5 M $KHCO_3$, and 15 L of 2 M KOH, respectively, while the anolytes were 500 mL of 5 M KOH, 1 L of 5 M KOH and 15 L of 2 M KOH, respectively.

During eCO_2RR, the catholytes used at the reactors with 100, 300 and 400 cm^2 GDEs were 5 L of 0.5 M $KHCO_3$, 15 L of 0.5 M $KHCO_3$ and 15 L of 2 M KOH respectively, while the anolytes were 1 L of 3 M KOH, 2 L of 3 M KOH and 15 L of 2 M KOH, respectively. The difference in the electrolyte composition at the largest scale (400 cm^2 GDE) compared to the smaller scales (100 and 300 cm^2 GDEs) was primarily due to the expected pH shift during eCO_2RR. As hydroxide ions are consumed during the reaction, pH shifts occur in the electrolyte solution.[11] This effect is anticipated to be more pronounced at larger scales because of the larger electrode surface area in contact with the catholyte. Therefore, 2 M KOH was used as both the catholyte and anolyte at the 400 cm^2 scale to maintain highly conductive and alkaline conditions in both electrochemical half-cells.

At the 100 and 300 cm^2 GDE reactors, all electrolyte solution inlets were positioned on one side, while the outlets were located on the opposite side. At the 400 cm^2 GDE reactors, however, the anolyte and catholyte solutions entered the reactors from the opposite sides. Nevertheless, this configuration did not impact the overall flow design of the catholyte and anolyte. A PTFE middle plate was installed at each solution inlet of 100 and 300 cm^2 GDE reactors to guide the flow into its respective chamber, ensuring that the electrolyte solution flows followed the intended paths. As a result, the final flow configuration was functionally equivalent to that used at the 400 cm^2 GDE reactor.

Before starting the experiments, $KHCO_3$ catholytes were purged with CO_2 until their pH reached a stable value (*ca.* 7.5 ± 2.0). The pH and conductivity of the anolyte at 100 and 300 cm^2 setups were measured periodically to make sure it sufficed for eCO_2RR. It was observed that 3 M KOH solution provided a highly alkaline (pH = 14) and conductive (>200 mS cm^{-1}) anolyte sufficient for eCO_2RR processes.

4.5 Analytical analyses

4.5.1 Liquid analyses at UFZ. High-performance liquid chromatography (HPLC, Shimadzu Scientific Instruments, USA) was used to analyse the collected liquid samples during the experiments. HPLC was equipped with a refractive index detector (RID) (RID-20A, Shimadzu Scientific Instruments, Japan) and Hi-Plex H column (300 mm × 7.7 mm ID, 8 μm pore size, Agilent Technologies, Germany) with a pre-column (Carbo-H 4 mm × 3 mm ID, Security Guard, Phenomenex). Isocratic elution was performed with 0.005 M H_2SO_4 at 0.5 mL min^{-1} at 50 °C for 30 min^{-1}. Formate calibration (1.14 mM to 44.4 mM, five-point calibration with triplicate standards for each point, R^2 = 0.99) was carried out with external standards, since formate was the only product in the liquid phase.

When required the inorganic carbon within the catholyte solution was measured using a total inorganic carbon analyser (TOC-L, Shimadzu, Japan), after addition of diluted phosphoric acid at room temperature and measurement of

the evolved CO_2 *via* a non-dispersive infrared (NDIR) detector.

4.5.2 Gas analyses at UFZ. Two channels from a four-channel micro GC equipped with a thermal conductivity detector (GC-TCD) was used to analyse the gas composition during eCO_2RR, as described before.[27] In all the experiments, the gas outlet port from the catholyte tank was connected to a N_2-mass flow meter/controller (MFM; LOW-Δ*P*-FLOW F-101D, 60 mLn min^{-1}, Bronkhorst High-Tech B.V., Ruurlo, Netherlands) controlled by a Flow-Bus (Bronkhorst High-Tech B.V., Ruurlo, Netherlands) with a micro GC (3000 Micro GC, INFICON, Cologne, Germany) in by-pass in order to determine the gas composition after calibrating the micro GC for O_2, H_2, N_2, CO_2 and CO detection, and their volume. The detailed information of the method used with the micro-GC-TCD is summarized in Table S1.† Gas measurements were carried out at the beginning of the eCO_2RR (t_0) and every 30 min during the experiment.

The gas volume $v^{norm}_{measured}$ was recorded in mLn using the mass flow meter and the mole fraction y_i of each individual gas component i [%] was obtained from the micro GC-TCD measurement, as explained previously.[32]

4.5.3 Liquid analyses at VITO. The collected liquid samples were also analysed by HPLC. An Agilent 1200 High-Performance Liquid Chromatograph with an Agilent Hi-Plex H 7.7 × 300 mm column was used to separate the product, and an Agilent 1260 RID detector was used to detect and quantify the formate in the form of formic acid. The samples were previously diluted with water and acidified with H_2SO_4 to avoid bubble formation and obstruction in the column. 0.01 M H_2SO_4 was used as the mobile phase.

4.6 Electrode analyses

4.6.1 Scanning electron microscopy (SEM) images and energy dispersive X-ray spectroscopy (EDX) at VITO. SEM images were taken using a Phenom ProX Desktop SEM designed by Thermo Fischer Scientific. It is equipped with a long-lifetime CeB6 source and integrates SEM and EDS functions into a single interface. It has a light optical magnification of 27–160× and an electron optical magnification range of 160–350 000×. It offers a resolution of 6 nm SED and 8 nm BSD. The accelerator voltages can be adjusted between 5 kV and 15 kV (4.8 kV and 20.5 kV in the advanced mode), and it can accommodate a sample size of up to 25 nm in diameter (optional 32 nm) and up to 35 mm in height (optional 100 mm).

The EDX (energy dispersive X-ray spectroscopy) analysis was performed using a Nimnici silicon drift detector (SDD) integrated into a Phenom Desktop SEM. The detector has a 25 mm^2 active area equipped with an ultra-thin silicon nitride (SiNx) X-ray window. It provides an energy resolution of ≤132 eV (Mn K_α) and operates with 2048 channels at 10 eV Ch^{-1}, with a maximum input count rate of 300 000 counts per second (cps). Fully embedded in the SEM, the system requires no external beam control.

4.7 Calculations

For each replicate, the values were calculated according to the equations below, and the average and standard deviation for each condition are reported in the manuscript.

4.7.1 Formate production rate (r_{HCOO^-}). r_{HCOO^-} was calculated based on the amount of formate produced (n_{HCOO^-}) between sampling points (dt) using eqn (1).

$$r_{HCOO^-}\left(\text{mM h}^{-1}\right) = \frac{n_{HCOO^-}}{dt} \quad (1)$$

4.7.2 Coulombic efficiency (CE). CE was calculated using eqn (2), considering the theoretical charge required for production of each compound (Q_i) and the experimentally supplied charge (Q_{total}) by DC power supply:

$$CE_i = \frac{Q_i}{Q_{total}} \times 100\% = \frac{n_i \times z_i \times F}{\int i(t)dt} \times 100\% \quad (2)$$

where n_i is the amount of each substance produced in mol, z_i is the number of transferred electrons per molecule and F = 96.485 C mol^{-1} is the Faraday constant. n_i is the difference between the concentration of each product within sampling times, measured by micro-GC-TCD or HPLC. z_i is 2 for all the products according to eqn (3)–(5) under alkaline or neutral conditions used in this study.

Under alkaline or neutral conditions:

$$CO_2 + H_2O + 2e^- \rightarrow HCOO^- + OH^- \quad (3)$$

$$CO_2 + H_2O + 2e^- \rightarrow CO + 2OH^- \quad (4)$$

$$2H_2O + 2e^- \rightarrow H_2 + 2OH^- \quad (5)$$

4.7.3 Carbon conversion efficiency (CCE). When required, CCE was calculated using the molar amount of carbon that was found in all the products ($\sum n_{C\_products}$) detected by HPLC and micro-GC-TCD, and the molar amount of carbon that was consumed as the substrate ($\sum n_{C\_substrate}$) according to eqn (6):

$$CCE = \frac{\sum n_{C\_products}}{\sum n_{C\_substrate}} \times 100\% \quad (6)$$

$\sum n_{C\_substrate}$ was the combination of the carbon provided in the form of bicarbonate in the catholyte measured by TIC, as well as the amount of carbon within the gaseous CO_2 fed during the experiment. The mol of CO_2(n) was calculated using ideal gas law (eqn (7)):

$$p \times V = n \times R \times T \quad (7)$$

where p is 1 bar as adjusted in the experiments, V is the volume of the gas depending on the adjusted flow rate during 120 min in L, R = 0.083144598 L bar mol^{-1} K^{-1} is a gas constant, and T is a temperature in K. The accuracy of

the CO_2 calculation was also confirmed by measuring the CO_2 provided for 120 min using the mass flow meter (MFM; LOW-Δ*P*-FLOW F-101D, 60 mLn min^{-1}, Bronkhorst High-Tech B.V., Ruurlo, Netherlands).

Data availability

The data supporting this article have been included as part of the ESI.†

Author contributions

P. I. – conceptualisation, investigation, methodology, data curation, visualisation, writing – original draft, review and editing, supervision. S. V. – conceptualisation, investigation, methodology, data curation, formal analysis, visualisation, validation, writing – review and editing. C. S. – methodology, formal analysis, validation, visualisation. P. H. – methodology, formal analysis, validation. C. S. – conceptualisation, investigation, methodology, data curation, writing – review and editing. A. G. – methodology, formal analysis, validation, visualisation, writing – review and editing. D. P. – conceptualisation, investigation, writing – review and editing, supervision, funding acquisition. F. H. conceptualisation, investigation, writing – review and editing, supervision, funding acquisition.

Conflicts of interest

The author Deepak Pant is inventor on the patent application EP4182491A1 "Carbon free gas diffusion electrode" (filed in 2020) while authors Chandani Singh and Deepak Pant are inventors on the patent application EP23177314.4 "Re-activation process of gas diffusion electrode" nfiled in 2023) and thus declare a competing financial interest due to employment at VITO. The other authors have no competing financial interests.

Acknowledgements

The authors acknowledge the support of the VIVALDI project that has received funding from the European Union's Horizon 2020 research and innovation programme under grant agreement 101000441. This work was supported by the Helmholtz-Association in the frame of the Integration Platform "Tapping nature's potential for sustainable production and a healthy environment" at the UFZ. A. G. and D. P. also acknowledge the support from the European Union's Horizon 2021 programme under the Marie Skłodowska-Curie Doctoral Networks (MSCA-DN) grant agreement No 101072830 (ECOMATES).

References

1 Y. Song, J. R. Junqueira, N. Sikdar, D. Öhl, S. Dieckhöfer, T. Quast, S. Seisel, J. Masa, C. Andronescu and W. Schuhmann, B-Cu-Zn gas diffusion electrodes for CO_2 electroreduction to C_{2+} products at high current densities, *Angew. Chem., Int. Ed.*, 2021, **60**, 9135–9141.

2 C. P. O'Brien, R. K. Miao, A. Shayesteh Zeraati, G. Lee, E. H. Sargent and D. Sinton, CO_2 electrolyzers, *Chem. Rev.*, 2024, **124**, 3648–3693.

3 S. Mukhopadhyay, M. S. Naeem, G. Shiva Shanker, A. Ghatak, A. R. Kottaichamy, R. Shimoni, L. Avram, I. Liberman, R. Balilty and R. Ifraemov, Local CO_2 reservoir layer promotes rapid and selective electrochemical CO_2 reduction, *Nat. Commun.*, 2024, **15**, 3397.

4 Y. Y. Birdja, E. Pérez-Gallent, M. C. Figueiredo, A. J. Göttle, F. Calle-Vallejo and M. T. Koper, Advances and challenges in understanding the electrocatalytic conversion of carbon dioxide to fuels, *Nat. Energy*, 2019, **4**, 732–745.

5 B. Belsa, L. Xia and F. P. García de Arquer, CO_2 electrolysis technologies: Bridging the gap toward scale-up and commercialization, *ACS Energy Lett.*, 2024, **9**, 4293–4305.

6 B. S. Crandall, B. H. Ko, S. Overa, L. Cherniack, A. Lee, I. Minnie and F. Jiao, Kilowatt-scale tandem CO_2 electrolysis for enhanced acetate and ethylene production, *Nat. Chem. Eng.*, 2024, **1**, 421–429.

7 G. G. Botte, Electrochemical manufacturing in the chemical industry, *Electrochem. Soc. Interface*, 2014, **23**, 49.

8 M. Orlić, C. Hochenauer, R. Nagpal and V. Subotić, Electrochemical reduction of CO_2: A roadmap to formic and acetic acid synthesis for efficient hydrogen storage, *Energy Convers. Manage.*, 2024, **314**, 118601.

9 V. Chanda, D. Blaudszun, L. Hoof, I. Sanjuán, K. Pellumbi, K. Junge Puring, C. Andronescu and U. P. Apfel, Exploring the (dis)-similarities of half-cell and full cell zero-gap electrolyzers for the CO_2 electroreduction, *ChemElectroChem*, 2024, **11**, e202300715.

10 M. G. Kibria, J. P. Edwards, C. M. Gabardo, C. T. Dinh, A. Seifitokaldani, D. Sinton and E. H. Sargent, Electrochemical CO_2 reduction into chemical feedstocks: From mechanistic electrocatalysis models to system design, *Adv. Mater.*, 2019, **31**, 1807166.

11 S. Varhade, A. Guruji, C. Singh, G. Cicero, M. García-Melchor, J. Helsen and D. Pant, Electrochemical CO_2 reduction: Commercial innovations and prospects, *ChemElectroChem*, 2025, **12**, e202400512.

12 A. G. Fink, F. Navarro-Pardo, J. R. Tavares and U. Legrand, Scale-up of electrochemical flow cell towards industrial CO_2 reduction to potassium formate, *ChemCatChem*, 2024, **16**, e202300977.

13 J. P. Edwards, T. Alerte, C. P. O'Brien, C. M. Gabardo, S. Liu, J. Wicks, A. Gaona, J. Abed, Y. C. Xiao and D. Young, Pilot-scale CO_2 electrolysis enables a semi-empirical electrolyzer model, *ACS Energy Lett.*, 2023, **8**, 2576–2584.

14 I. Dutta, S. Chatterjee, H. Cheng, R. K. Parsapur, Z. Liu, Z. Li, E. Ye, H. Kawanami, J. S. C. Low and Z. Lai, Formic acid to power towards low-carbon economy, *Adv. Energy Mater.*, 2022, **12**, 2103799.

15 K. Van Daele, B. De Mot, M. Pupo, N. Daems, D. Pant, R. Kortlever and T. Breugelmans, Sn-based electrocatalyst stability: A crucial piece to the puzzle for the electrochemical CO_2 reduction toward formic acid, *ACS Energy Lett.*, 2021, **6**, 4317–4327.

16 D. A. Bulushev and J. R. Ross, Towards sustainable production of formic acid, *ChemSusChem*, 2018, **11**, 821–836.
17 R. Bhaskaran, B. G. Abraham and R. Chetty, Recent advances in electrocatalysts, mechanism, and cell architecture for direct formic acid fuel cells, *WIREs Energy Environ.*, 2022, **11**, e419.
18 G. A. El-Nagar, M. A. Hassan, I. Lauermann and C. Roth, Efficient direct formic acid fuel cells (DFAFCs) anode derived from seafood waste: Migration mechanism, *Sci. Rep.*, 2017, **7**, 17818.
19 C. Zhang, X. Hao, J. Wang, X. Ding, Y. Zhong, Y. Jiang, M. C. Wu, R. Long, W. Gong and C. Liang, Concentrated formic acid from CO_2 electrolysis for directly driving fuel cell, *Angew. Chem., Int. Ed.*, 2024, **136**, e202317628.
20 P. Izadi and F. Harnisch, Microbial| electrochemical CO_2 reduction: To integrate or not to integrate?, *Joule*, 2022, **6**, 935–940.
21 P. Izadi, A. Kas, P. Haus and F. Harnisch, On the stability of electrochemical CO_2 reduction reaction to formate at indium electrodes at biocompatible conditions, *Electrochim. Acta*, 2023, **462**, 142733.
22 K. Fernández-Caso, G. Díaz-Sainz, M. Alvarez-Guerra and A. Irabien, Electroreduction of CO_2: Advances in the continuous production of formic acid and formate, *ACS Energy Lett.*, 2023, **8**, 1992–2024.
23 D. Song, S. Zhang, M. Zhou, M. Wang, R. Zhu, H. Ning and M. Wu, Advances in the stability of catalysts forelectroreduction of CO_2 to formic acid, *ChemSusChem*, 2024, **17**, e202301719.
24 C. Singh, J. Song, J. Radomski, Z. Chen, Y. Y. Birdja, J. Vaes and D. Pant, Re-activation process of gas diffusion electrode, *EU Pat.*, EP4474526A1, 2024.
25 J. A. Abarca, M. Coz-Cruz, M. Alvarez-Guerra, G. Díaz-Sainz and A. Irabien, Experimental assessment of different reactor configuration approaches for direct CO_2 electroreduction to formic acid, *Electrochim. Acta*, 2025, **525**, 146182.
26 B. Jacobs, D. Pant, D. Van Houtven, M. Erwin, J. Vaes and Y. Y. Birdja, Carbon free gas diffusion electrode, *U.S. Pat.*, Application 18/014,827, 2023.
27 P. Izadi, J. Song, C. Singh, D. Pant and F. Harnisch, Assessing the electrochemical CO_2 reduction reaction performance requires more than reporting coulombic efficiency, *Adv. Energy Sustainability Res.*, 2024, **5**, 2400031.
28 A. S. Agarwal, E. Rode, D. Hill, S. Guan and N. Sridhar, Electrochemical conversion of CO_2 to useful products, *J. Electrochem. Soc.*, 2013, 699.
29 K. Fan, Y. Jia, Y. Ji, P. Kuang, B. Zhu, X. Liu and J. Yu, Curved surface boosts electrochemical CO_2 reduction to formate via bismuth nanotubes in a wide potential window, *ACS Catal.*, 2019, **10**, 358–364.
30 W. Li, C. Yu, X. Tan, Y. Ren, Y. Zhang, S. Cui, Y. Yang and J. Qiu, Beyond leverage in activity and stability toward CO_2 electroreduction to formate over a bismuth catalyst, *ACS Catal.*, 2024, **14**, 8050–8061.
31 F. Bienen, A. Löwe, J. Hildebrand, S. Hertle, D. Schonvogel, D. Kopljar, N. Wagner, E. Klemm and K. A. Friedrich, Degradation study on tin-and bismuth-based gas-diffusion electrodes during electrochemical CO_2 reduction in highly alkaline media, *J. Energy Chem.*, 2021, **62**, 367–376.
32 K. Neubert, M. Hell, M. Chávez Morejón and F. Harnisch, Hetero-coupling of bio-based medium-chain carboxylic acids by kolbe electrolysis enables high fuel yield and efficiency, *ChemSusChem*, 2022, **15**, e202201426.
33 L.-X. Liu, Y. Zhou, Y.-C. Chang, J.-R. Zhang, L.-P. Jiang, W. Zhu and Y. Lin, Tuning Sn_3O_4 for CO_2 reduction to formate with ultra-high current density, *Nano Energy*, 2020, **77**, 105296.
34 J. Wang, S. Ning, M. Luo, D. Xiang, W. Chen, X. Kang, Z. Jiang and S. Chen, In-Sn alloy core-shell nanoparticles: In-doped SnO_x shell enables high stability and activity towards selective formate production from electrochemical reduction of CO_2, *Appl. Catal., B*, 2021, **288**, 119979.
35 A. J. Welch, A. Q. Fenwick, A. Bohme, H.-Y. Chen, I. Sullivan, X. Li, J. S. DuChene, C. Xiang and H. A. Atwater, Operando local pH measurement within gas diffusion electrodes performing electrochemical carbon dioxide reduction, *J. Phys. Chem. C*, 2021, **125**, 20896–20904.
36 T. Wu, H. Bu, S. Tao and M. Ma, Determination of local pH in CO 2 electroreduction, *Nanoscale*, 2024, **16**, 3926–3935.
37 A. Somoza-Tornos, O. J. Guerra, A. M. Crow, W. A. Smith and B.-M. Hodge, Process modeling, techno-economic assessment, and life cycle assessment of the electrochemical reduction of CO2: A review, *iScience*, 2021, **24**, 102813.
38 A. S. Agarwal, Y. Zhai, D. Hill and N. Sridhar, The electrochemical reduction of carbon dioxide to formate/formic acid: Engineering and economic feasibility, *ChemSusChem*, 2011, **4**, 1301–1310.
39 H. Yang, J. J. Kaczur, S. D. Sajjad and R. I. Masel, Electrochemical conversion of CO_2 to formic acid utilizing Sustainion™ membranes, *J. CO_2 Util.*, 2017, **20**, 208–217.
40 A. Del Castillo, M. Alvarez-Guerra, J. Solla-Gullón, A. Sáez, V. Montiel and A. Irabien, Sn nanoparticles on gas diffusion electrodes: Synthesis, characterization and use for continuous CO_2 electroreduction to formate, *J. CO_2 Util.*, 2017, **18**, 222–228.
41 G. Díaz-Sainz, M. Alvarez-Guerra, J. Solla-Gullón, L. García-Cruz, V. Montiel and A. Irabien, CO_2 electroreduction to formate: Continuous single-pass operation in a filter-press reactor at high current densities using Bi gas diffusion electrodes, *J. CO2 Util.*, 2019, **34**, 12–19.
42 Y. Chen, A. Vise, W. E. Klein, F. C. Cetinbas, D. J. Myers, W. A. Smith, T. G. Deutsch and K. C. Neyerlin, A robust, scalable platform for the electrochemical conversion of CO_2 to formate: Identifying pathways to higher energy efficiencies, *ACS Energy Lett.*, 2020, **5**, 1825–1833.
43 S. Hao, A. Elgazzar, N. Ravi, T.-U. Wi, P. Zhu, Y. Feng, Y. Xia, F.-Y. Chen, X. Shan and H. Wang, Improving the operational stability of electrochemical CO_2 reduction reaction via salt precipitation understanding and management, *Nat. Energy*, 2025, 1–12.

44 Y. Zhang, D. Yao, J. Liu, Z. Wang and L. Wang, Advancing strategies on green H_2 production via water electrocatalysis: Bridging the benchtop research with industrial scale-up, *Microstructures*, 2024, **4**, 2024020.

45 F. Meharban, C. Lin, X. Wu, L. Tan, H. Wang, W. Hu, D. Zhou, X. Li and W. Luo, Scaling up stability: Navigating from lab insights to robust oxygen evolution electrocatalysts for industrial water electrolysis, *Adv. Energy Mater.*, 2024, **14**, 2402886.